



## OPEN ACCESS

## EDITED BY

Rui Wang,  
Northeastern University, China

## REVIEWED BY

Adriano Chaves Lisboa,  
Solutions on demand, Brazil  
Xuguang Hu,  
Northeastern University, China

## \*CORRESPONDENCE

Xingxing Han,  
✉ hanxx@hhu.edu.cn

RECEIVED 27 July 2023

ACCEPTED 17 October 2023

PUBLISHED 09 November 2023

## CITATION

Xu C, Jiao Z, Han X, Huang Y, Wang J,  
Zhang H and Shen WZ (2023),  
Comprehensive layout optimization of  
the transmission system in a deepwater  
wind farm cluster.  
*Front. Energy Res.* 11:1268291.  
doi: 10.3389/fenrg.2023.1268291

## COPYRIGHT

© 2023 Xu, Jiao, Han, Huang, Wang,  
Zhang and Shen. This is an open-access  
article distributed under the terms of the  
[Creative Commons Attribution License  
\(CC BY\)](#). The use, distribution or  
reproduction in other forums is  
permitted, provided the original author(s)  
and the copyright owner(s) are credited  
and that the original publication in this  
journal is cited, in accordance with  
accepted academic practice. No use,  
distribution or reproduction is permitted  
which does not comply with these terms.

# Comprehensive layout optimization of the transmission system in a deepwater wind farm cluster

Chang Xu<sup>1</sup>, Zhixiong Jiao<sup>1</sup>, Xingxing Han<sup>1\*</sup>, Yuwei Huang<sup>1</sup>,  
Jincheng Wang<sup>1</sup>, Hu Zhang<sup>1</sup> and Wen Zhong Shen<sup>2</sup>

<sup>1</sup>College of Energy and Electrical Engineering, Hohai University, Nanjing, China, <sup>2</sup>College of Electrical, Energy and Power Engineering, Yangzhou University, Yangzhou, China

Compared to nearshore wind farms, deepwater offshore wind farms have better wind resources and broader development space and will be the main trend of wind power development in the future. Due to the long distance from the shore, the investment and operation costs of the transmission system in a deepwater wind farm cluster are high and the electricity generated by the cluster is commonly transmitted by high-voltage direct current transmission technology to decrease power losses. For a given converter station, the comprehensive optimization of the layouts of the substations, AC export cables from the substation to the converter station, and cable arrays within each wind farm are complex and have not been well studied. This paper proposes a multi-level nested optimization strategy to minimize the total cost of the collection cables for a deepwater offshore wind farm cluster. The proposed method applies the Informed-RRT\* method to optimize the layout of AC export cables while the cable arrays are arranged by Prim's algorithm. During the optimization process, the gradient descent algorithm is used to optimize the positions of the substations, obtaining the transmission system scheme with the minimum cable investment. For a certain deepwater wind farm cluster, the total cable cost after optimization is reduced by 3.58%, which indicates the effectiveness of this method.

## KEYWORDS

deepwater, wind farm cluster, transmission system, the gradient descent algorithm, Informed-RRT\* method

## 1 Introduction

Offshore wind energy has the advantages of large reserves, high power density, stable wind speeds, and proximity to load centers. The offshore wind power of China has experienced rapid development in recent years, with an added capacity of 5.16 GW and a cumulative installed capacity of 30.51 GW in 2022 ([Global Wind Energy Council, 2022](#)). The exploitable potential of deepwater wind power in China is estimated to be approximately 1582 GW, which is much larger than that in nearshore areas ([World Bank Group, 2020](#)). Furthermore, the development of deepwater wind power faces fewer constraints and offers greater development space, making it suitable for large-scale concentrated development.

Compared to the widely used high-voltage alternating current (HVAC) transmission, high-voltage direct current (HVDC) transmission without reactive loss has significant technical and economic advantages, particularly for long-distance transmission in

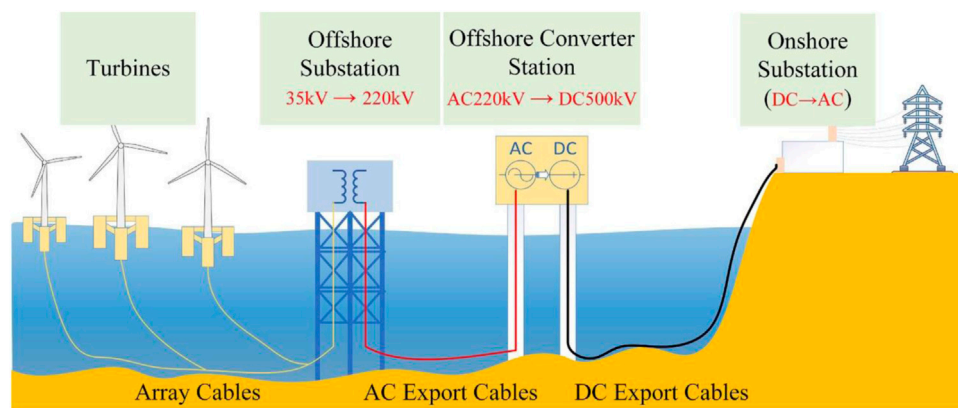


**FIGURE 1**  
Schematic diagram of power conversion of the deepwater wind farm cluster.

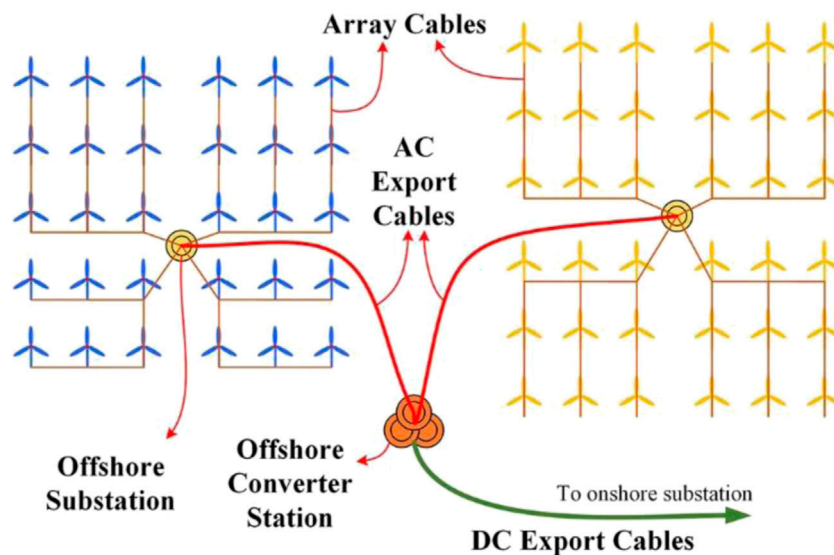


**FIGURE 2**  
Schematic diagram of the offshore wind farm cluster's transmission system.

deepwater offshore wind farm clusters (Fischetti and Pisinger, 2018; Liu et al., 2020). The offshore wind farm cluster transmission system (OWFCTS) is illustrated in Figure 1 and Figure 2. The electricity generated by wind turbines is first boosted at the offshore substation, transmitted through high-voltage AC cables (AC export cables) to the offshore converter station, rectified into high-voltage direct current, and then, transmitted via high-voltage DC cables (DC export cables) to the onshore substation. Based on the experience of nearshore wind farms, the investment in the offshore wind farm transmission system (offshore substation + array cable lines + AC export cables) accounts for over 15% of the total wind farm investment (Yang et al., 2022). As a deepwater wind farm cluster has a longer distance from the shore, the proportion of investment in the transmission system will further increase. Therefore, optimizing

the path of the transmission system can effectively reduce the investment cost of offshore wind power.

The design of the transmission system for offshore wind farm cluster is an integrated optimization problem that can be divided into three layers: (1) optimization for the offshore substation location, (2) path optimization for the array cables in the wind farm, and (3) path optimization for the AC export cables connecting the substation and the converter station. Before optimizing the OWFCTS comprehensively, the planned capacity of the wind farm needs to be determined. Rui Wang et al. proposed an accurate current sharing and voltage regulation based on the distributed adaptive dynamic programming approach in a power grid with a wind farm, which could control the variable and achieve accurate current to protect the power grid (Wang et al., 2022). Wang

Rui et al. proposed the guardian map theory based on the Kronecker sum regarding the impedance-based approach in polar coordinates, which guides the system obtaining wind farm planning and stabilization method research (Wang et al., 2020). In terms of the optimization of the offshore substation location, Won-Sik Moon et al. employed a genetic algorithm to optimize the location to minimize the overall cost (Moon et al., 2014). Peng Hou et al. used an exhaustive search method to find the optimal location for the substation (Hou et al., 2015). Je-Seok Shin et al. introduced a methodology to design an optimal cable layout of the inner grid as well as the location of the offshore substation (Shin and Kim, 2016). Mokhi et al. compared the effectiveness of particle swarm optimization and genetic algorithm in optimizing the substation location and found that the particle swarm optimization algorithm yielded faster optimal results but had the issue of uneven loop division in the collection lines (El Mokhi and Addaim, 2020). Yang et al. 2020 searched for the location with the minimum cost for the substation along a straight line between the centroid of the wind farm and the point with the minimum offshore distance. They found that the booster station location was primarily influenced by the price of AC export cables, where a higher cable price resulted in a closer offshore location for the substation. However, this research did not prove that the global optimum value could be obtained on this straight line (Yang et al., 2022). Regarding the optimization of the collection line path, it is common to divide the circuits using k-means clustering (Shin and Kim, 2016) or fuzzy C-means clustering (Zuo et al., 2019) and then connect the cables with the shortest path using the minimum spanning tree (MST) method. Cazzaro D et al. encoded the positions of the wind turbines and substations and used a heuristic algorithm to optimize the path of the collection lines (Cazzaro et al., 2020). Fischetti M and Ulku I transformed the topological structure of the wind farm collection lines into a mixed-integer linear programming (MILP) model for optimization and solution (Fischetti and Pisinger, 2018; Ulku and Alabas-Uslu, 2020). The HVDC transmission system, as compared to the HVAC transmission system, requires the inclusion of converter stations. The cost of cables exhibits an exponential relationship with transmission capacity (Lundberg et al., 2003). Hence, as the capacity of the offshore wind farm increases, the transmission system cost also experiences a significant increase. Typically, the locations of wind turbines and converter stations in a deepwater offshore wind farm cluster are selected first. By optimizing the locations of offshore substations and the length of transmission cables, the investment in the wind farm can be minimized. The deepwater offshore wind farm cluster with HVDC transmission systems is the future trend of offshore wind power. However, there is limited research focusing on the optimization of transmission systems. This paper proposes an integrated optimization method to optimize the path of the transmission system in a deepwater offshore wind farm cluster in three steps: array cable optimization, substation location optimization, and AC export cable path optimization. In particular, the array cables are independently optimized within the wind farm, whereas the AC export cables need to be cooperatively optimized across multiple wind farms to prevent cable cross, which could simplify the complexity associated with optimizing the wind

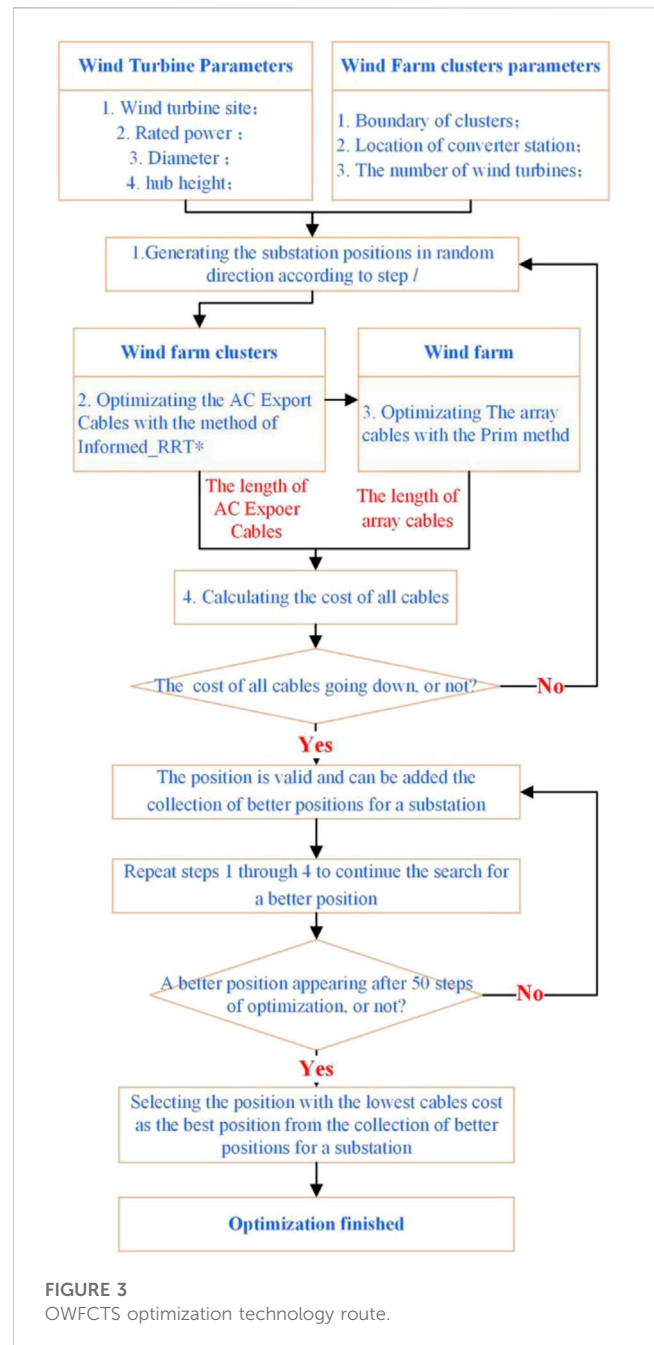
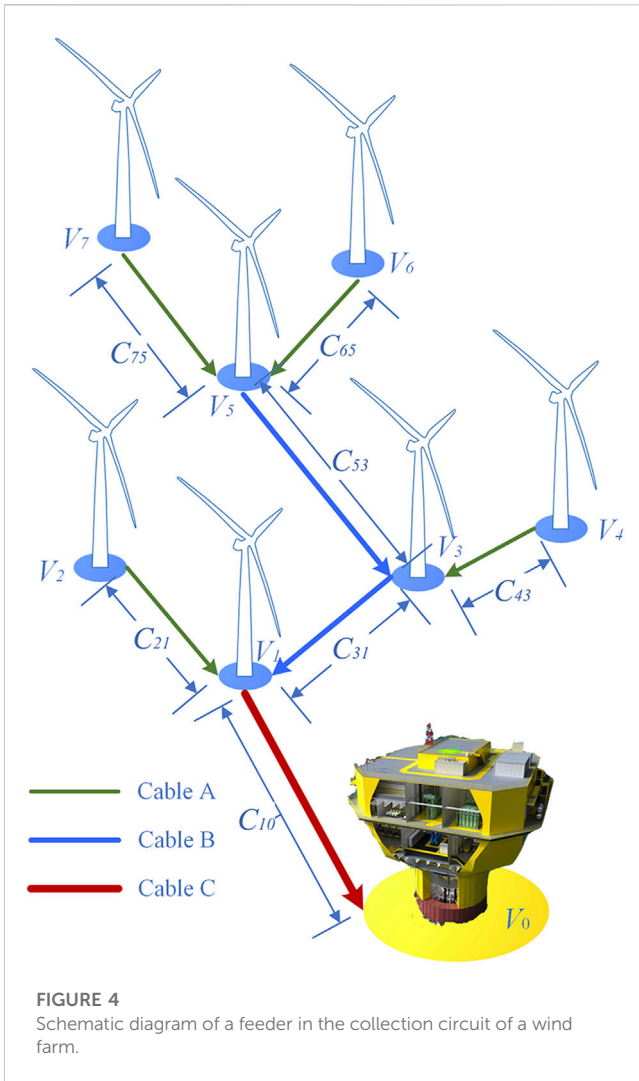


FIGURE 3 OWFCTS optimization technology route.

farm’s transmission system. Finally, a validation case on the wind farm cluster in a certain sea area is presented.

## 2 OWFCTS optimization model

In this paper, the locations of wind farm substations are adapted by a gradient descent algorithm in the direction of a decreasing transmission system cable cost gradient while an inner optimization of AC export cable paths and array cables is carried out. Figure 3 shows the algorithmic flow of this method. Initially, the position of the substation is randomly generated around the geometric center of the wind farm. Based on this position, we use the Informed-RRT\* method (Gammell et al., 2014) described in Section 2.2 to optimize the AC



$$OWFCTS = \{(G_1(V, A), EC_1), (G_2(V, A), EC_2), \dots, (G_i(V, A), EC_i)\}, \tag{1}$$

$$G(V, A) = \{g_1(V, A), g_2(V, A), \dots, g_j(V, A)\}, \tag{2}$$

$$V = \{V_0, V_1, V_2, \dots, V_k\}, \tag{3}$$

$$A = \{A_{01}, A_{12}, A_{23}, \dots, A_{01}\} \\ m, n \in \{1, 2, \dots, k\}, m \neq n, \tag{4}$$

where  $EC_i$  is an AC export cable;  $G(V, A)$  is the set of array cables of the wind farm, which consist of several feeders  $g(V, A)$ , where  $V$  represents the vertex on each feeder,  $V_0$  is the substation at the end of the feeder, and  $V_1 \sim V_k$  stand for wind turbines;  $A$  is the set of the length of array cables; and  $A_{mn}$  is the length of the cable from turbine  $m$  to turbine  $n$ .

## 2.2 Optimization objective function

The OWFCTS generally uses several types of cables for economic reasons. The price of cables  $P$  is shown in Eq. 5, and  $C_{mn}$  (Eq. 6) is the cost of the cable from turbine  $m$  to turbine  $n$ . Figure 4 represents the array cables of any feeder in a wind farm, and the topology is represented, as shown in Eq. 7. To express a clear representation of the distribution of the cable cost of the OWFCTS, this paper introduces the degree matrix  $D$  to represent the cost of each segment of the cable in the wind farm. The elements in the degree matrix  $D$  are related to the weight matrix  $W$ , where  $D_i = W_{i1} + W_{i2} + \dots + W_{ij}$ . The traces of the matrix  $\text{tr}(D)$  which is the sum of the absolute values of the diagonal elements of the matrix in Eq. 9 is the total cost of the cables of any feeders of the array cables. As shown in Eq. 10, the total cost of the array cables is the sum of the traces of the matrix of the individual feeder. As shown in Eq. 11, the total cable cost of the OWFCTS is the sum of the cable cost of the array cables of the wind farms and the cost of the AC export cables, where  $Cost_i(G_i(V, A))$  is related to the cable section areas and the length of the array cables. The cable section areas are first selected via the maximum long-term operating current method in Section 2.3 and then checked by the voltage drop. The cable length is obtained by the optimization of the Prim method.  $Cost_i(EC_i)$  is related to the path length of the AC export cables that is optimized by the Informed-RRT\* method presented in Section 2.2.

$$P = \{P_1, P_2, \dots, P_i\}, \tag{5}$$

$$C_{mn} = A_{mn} \cdot P_i, \tag{6}$$

$$g(V, C) = \begin{cases} V = \{V_1, V_2, V_3, V_4, V_5, V_6, V_7\} \\ C = \{C_{10}, C_{21}, C_{31}, C_{43}, C_{53}, C_{65}, C_{75}\} \end{cases}, \tag{7}$$

$$W = \begin{bmatrix} 0 & 0 & 0 & 0 & 0 & 0 & 0 & 0 \\ C_{10} & 0 & 0 & 0 & 0 & 0 & 0 & 0 \\ 0 & C_{21} & 0 & 0 & 0 & 0 & 0 & 0 \\ 0 & C_{31} & 0 & 0 & 0 & 0 & 0 & 0 \\ 0 & 0 & 0 & C_{43} & 0 & 0 & 0 & 0 \\ 0 & 0 & 0 & C_{53} & 0 & 0 & 0 & 0 \\ 0 & 0 & 0 & 0 & 0 & C_{65} & 0 & 0 \\ 0 & 0 & 0 & 0 & 0 & C_{75} & 0 & 0 \end{bmatrix}, \tag{8}$$

export cable paths and Prim's algorithm to optimize array cables, respectively. After each optimization step, the cost of all cables at that position is calculated and compared with the cable cost at the last position. If the cost decreases, the position is considered valid. Otherwise, we return to step 1. The optimization process for the substation position is called the gradient descent method, which is described in detail in Section 3.1. Prim's algorithm was extensively studied, and this paper adopts the research results of the work of Shin et al. to optimize the array cables (Shin and Kim, 2016). Specifically, the k-means clustering method based on genetic algorithms is used for the feeder division, followed by the Prim method to generate the topology of the array cables.

## 2.1 OWFCTS model

The topological structure of the array cables of the offshore wind farm cluster can be regarded as a directed graph. As a collection of wind farm array cables and AC export cables, the OWFCTS can be represented as follows:



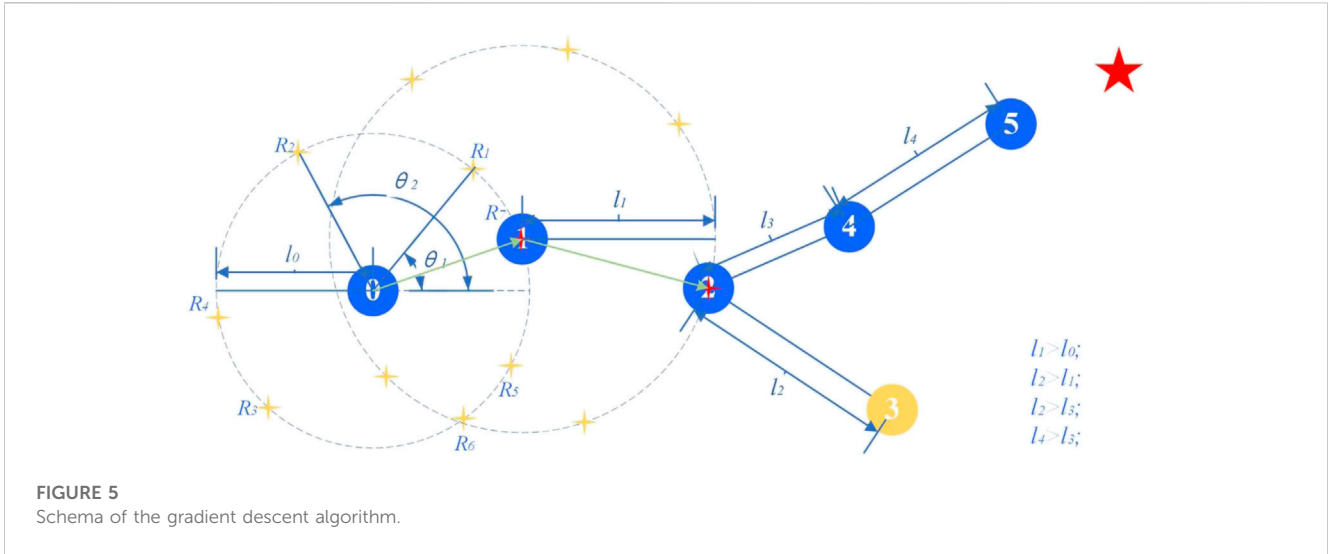


FIGURE 5 Schema of the gradient descent algorithm.

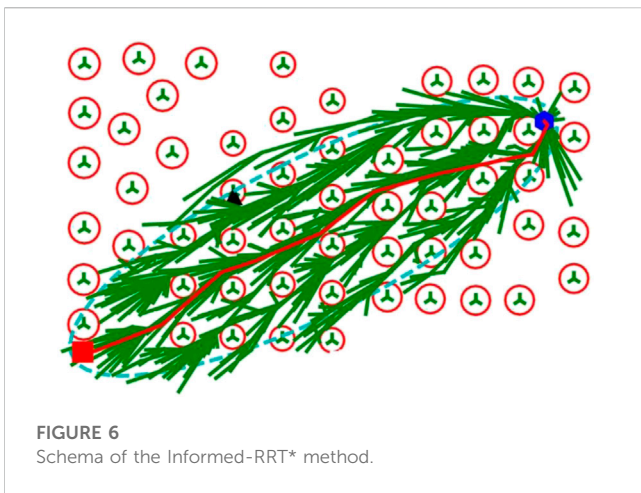


FIGURE 6 Schema of the Informed-RRT\* method.

path rather than an optimized path. The Informed-RRT\* algorithm improves on the RRT\* method in three ways (Gammell et al., 2014): (1) the Informed-RRT\* method first uses the RRT\* method to find a feasible path, and second, it takes the starting point and the endpoint as the focus of the ellipse, forming an ellipse that envelopes the first path, and then, the random points generated in subsequent searches are only within the ellipse; (2) the Informed-RRT\* method optimizes the path from the parent node to the new node after the new node is found; and (3) if the new node is randomly obtained to be on the side of the node start point of the already generated tree, the new node can be used to optimize the already generated tree and shorten the new node's length of tree branches within the range. The Informed-RRT\* method of searching the path is shown in Figure 6.

The main process of the Informed-RRT\* algorithm is as follows:

**Step 4:** Gradient descent algorithm optimization: Starting with this  $(x_2, y_2)$ , the optimization process produces two scenarios.

**Case 1:** With  $(x_2, y_2)$  as the starting point and  $l_2 = l_1 * k, k > 1$  as the step, we obtain the random point  $R_i(x_i, y_i)$ , and being able to find the point  $COST_i < COST_2$  is a good case to obtain  $(x_3, y_3)$ .

**Case 2:** If the method of Case 1 is used to search for 10 points and still no  $(x_3, y_3)$  is found, then the step size is modified to  $l_3 = l_2 * (1/k), k > 1$ , random points are generated, and the aforementioned steps are repeated to find  $(x_3, y_3)$ .

Step 4 is repeated; if no superior position appears after 50 optimal steps, OWFCTS optimization is accomplished.

### 3.2 AC export cable optimization based on the Informed-RRT\* method

The RRT algorithm is a sampling-based path planning method; however, due to the randomness of its sampling, it resulted in the final generated path that is often only a feasible

**Step 1:** Taking the location of the substation as the starting point  $(x_{start}, y_{start})$  of the randomized tree.

**Step 2:** Generating a random point  $(x_{rand}, y_{rand})$  within the whole wind farm area, the random point has a certain probability of being the location of the converter station  $(x_{end}, y_{end})$ .

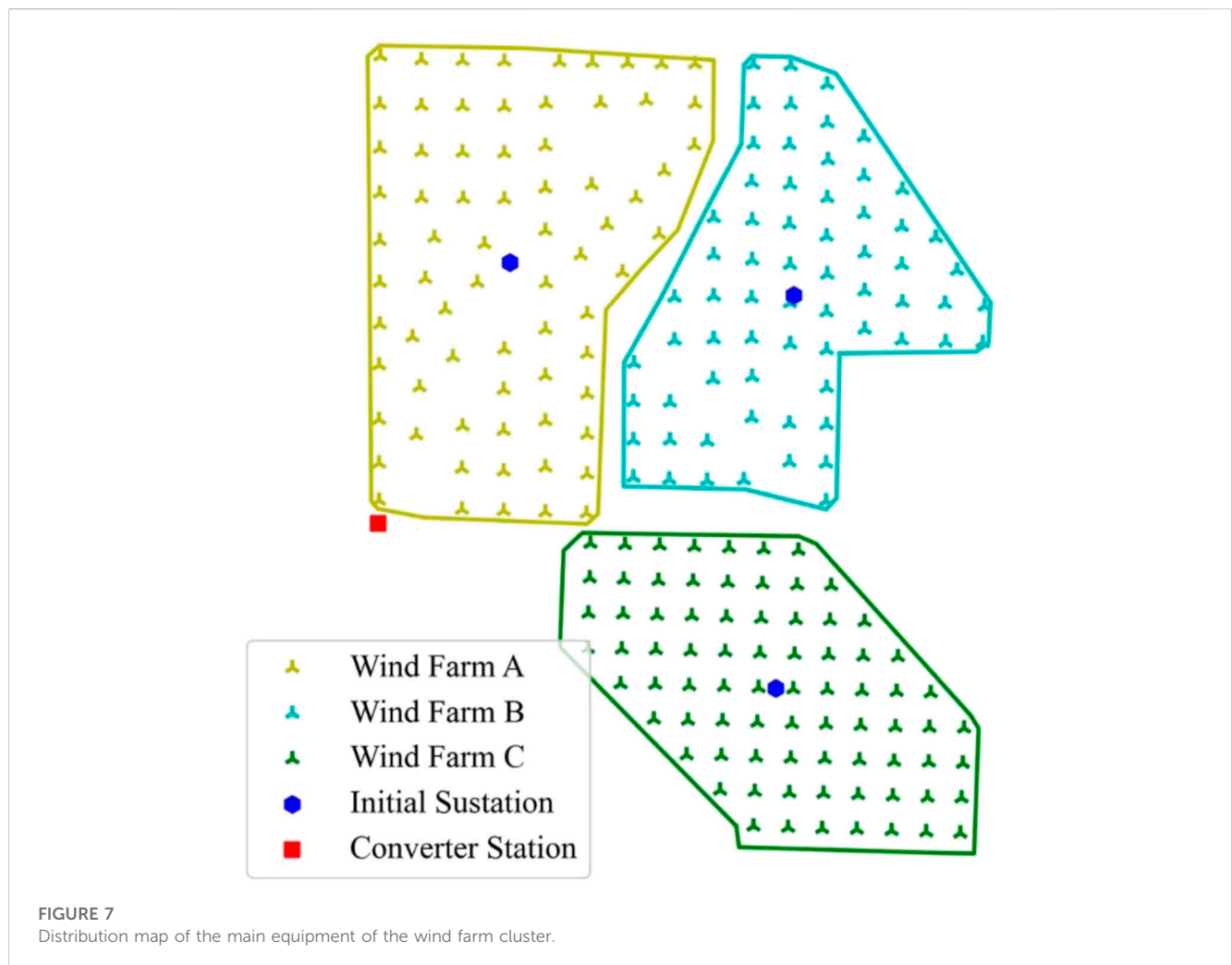
**Step 3:** Calculating the distance between each node in the random tree at this point and the generated random point  $(x_{rand}, y_{rand})$  and finding the nearest node to this random point, denoted as  $(x_{nearest}, y_{nearest})$ .

**Step 4:**  $(x_{nearest}, y_{nearest})$  is connected to  $(x_{rand}, y_{rand})$ , and then, it is determined whether this line segment intersects with an obstacle or a sensitive area; if it does not intersect, then this path is available; otherwise, we go back and re-select the random point  $(x_{rand}, y_{rand})$ .

**Step 5:** Optimizing the parent node of the new node  $(x_{new}, y_{new})$ : We search for the already generated nodes using a distance greater than the step size, and if there exists the point  $(x, y)$  such that the

TABLE 1 Information about wind farms.

Parameter	Wind farm A	Wind farm B	Wind farm C	Total
Number of wind turbines	40 + 32	66	78	216
Wind turbine-rated power	5MW/6.2 MW	6 MW	4 MW	\
Total capacity of the wind farm	398.4 MW	396 MW	312 MW	1106.4 MW
Wind turbine diameter	116m/152 m	150 m	120 m	\
Hub height	90m/110 m	100 m	90 m	\
Generator output voltage	690 V	690 V	690 V	\



path from  $(x, y)$  to  $(x_{new}, y_{new})$  is less than the path from  $(x, y)$  to  $(x_{nearest}, y_{nearest})$  and then to  $(x_{new}, y_{new})$ , and there is no intersection with the obstacle yet, then  $(x, y)$  is selected as the parent node of the new node  $(x_{new}, y_{new})$  to optimize the path.

**Step 6:** After the formation of a complete path through the aforementioned steps, the starting point and the endpoint serve as the vertices of the ellipse, generating an ellipse that encompasses the initial path, as shown in Figure 6, represented by the green line in the figure that is generated by the ellipse.

**Step 7:** continue to repeat steps 2 through 7, with the difference that the random points generated in step 2 are all within the ellipse. Optimization is continued until the number of optimizations reaches the set upper limit.

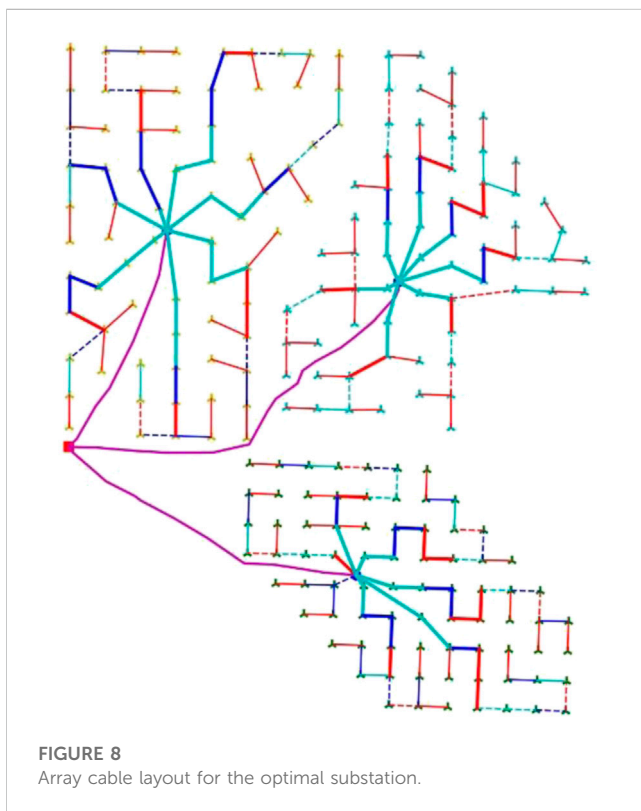
The obstacle to be avoided in the optimization is the wind turbine safety distance, which is defined as follows as shown by the red circle in Figure 6:

$$\text{Safety\_Dist} = 1.5 \cdot (H + 0.5D), \tag{18}$$

where  $H$  is the hub height of the wind turbine and  $D$  is the diameter.

TABLE 2 Wind farm cable parameters.

Type	Voltage level (kV)	Cross-sectional area (mm)	Minimum connection capacity (MW)	Maximum connection capacity (MW)	Unit price (CNY/meter)
Cable_A	35	50	0	7.5	1222
Cable_B	35	70	8	10.6	1331
Cable_C	35	95	12	14.3	1482
Cable_D	35	120	15	18.1	1663
Cable_E	35	150	19	22.7	1923
Cable_F	35	185	25	28	2290
Cable_G	35	240	32	36.3	3051
Cable_H	35	300	40	45.4	4245
Cable_I	35	400	55	60.6	7561
Cable_J	220	3*500	180	200	9388
Cable_K	220	3*1000	290	324	25417
Cable_L	220	3*1600	341	375	38545



### 4 Case study

The offshore wind farm cluster consists of three wind farms, with a total of 216 wind turbines and four types of turbines, whose total capacity is 1106.4 MW, as shown in Table 1. There is a converter station and three 220 kV offshore substations in the cluster. The layout of the turbines, substations, and converter stations in the wind farm cluster is shown in Figure 7. The blue dot in the figure represents the current

location of the substation of the wind farm, which is close to the geometric center of the wind farm, and is also the starting point of the optimization. The wind farm uses 35 kV array cables to connect the wind turbines to the substation and then converges to the converter station through a 220 kV AC export cable. Due to the large capacity of the wind farm, this case selects nine types of 35 kV cables and three types of 220 kV cables, whose cost is based on the research of Lundberg et al. (2003) and calculated by the maximum capacity transmitted by the cable. The calculation method is shown in Eq. 19. The parameter selection is shown in Supplementary Table S1, and the parameter information and cost of each cable are shown in Table 2. In the optimization, the positions of the wind turbines and the converter station are fixed, and the positions of the substations in each wind farm are optimized in the direction of cable cost gradient descent. The optimization results are shown in Sections 3.1 and 3.2.

$$Cost = A_p + B_p \exp\left(\frac{C_p S_n}{100}\right). \tag{19}$$

### 4.1 Overall optimization results

By using the optimization method and parameter selection proposed in this paper, an integrated optimization of OWFCTS is carried out. Figure 8 shows the layout of the cables and the location of the substation in the wind farm cluster after optimization. The comparison of cable length and cable cost before and after optimization is shown in Table 3. After optimization, the total length of array cables in the wind farm cluster is reduced by 319.79 m, a decrease of 0.17%; the path length of AC export cables is reduced by 5640.66 m, a decrease of 13.82%; and the total cable cost after optimization is reduced by 3.58%. The significant reduction in AC export cables is the main reason for the decrease in the total cable cost. As shown in Figure 9, in the path optimization of the OWFCTS, the total cost of the cable decreases the fastest when the number of optimization steps is between 0 and 40 because the original



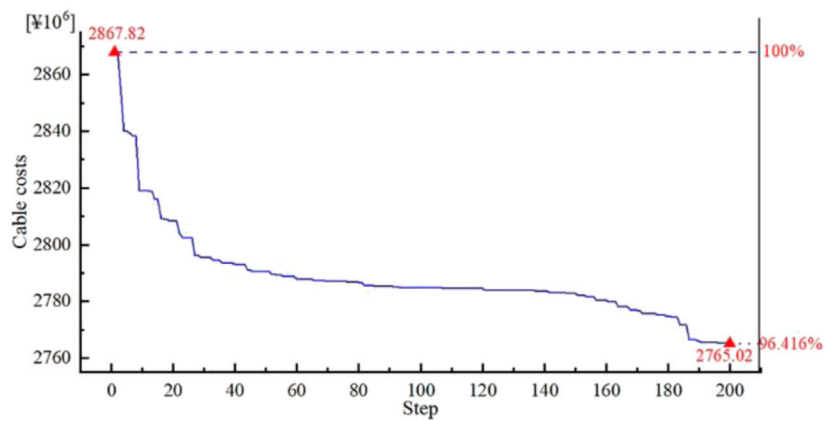


**FIGURE 9**  
Variation curve of total cable investment with the number of optimization steps in the OWFCTS.

**TABLE 3 Comparison of parameters before and after optimization of the OWFCTS.**

Quantities of the OWFCTS	Original substation location	Optimal substation location	Change
Length of array cables (m)	185900.42	185580.63	↓319.79
Length of AC export cables (m)	40824.84	35184.18	↓5640.66
Total cable cost (CNY*10 <sup>6</sup> )	2867.82	2765.02	↓102.80

**TABLE 4 Wind farm A optimization parameters.**

	Name	Value
Starting position	Length of AC export cables	9727.49 m
	Length of array cables	68958.03 m
	Total cable cost	940,476.9 *10 <sup>3</sup> CNY
	Line voltage drop	4.16%
Optimization parameter	Initial step size l0	200 m
	Number of optimization steps	200
Optimal position	Length of AC export cables	9083.71 m
	Length of array cables	68485.70 m
	Total cable cost	936,801.3 *10 <sup>3</sup> CNY
	Line voltage drop	4.25%
Changes	Change in the length of AC export cables	↓643.78 m
	Change in the length of array cables	↓472.33 m
	Change in the cable cost	↓3,675.7 *10 <sup>3</sup> CNY

location of the substation is not optimized, which leads to a large decrease in cable cost at the beginning of optimization. Between 40 and 180 steps, the gradient of cable cost decrease becomes smaller, and the optimization enters the bottleneck position. Between 180 and 200 steps, there is a small stepdown in cable cost, which is due to the use of random methods to jump out of the local optimum, and a relatively optimal substation location is found.

## 4.2 Optimization details for each wind farm

### 4.2.1 Optimization results of wind farm A

Wind farm A consists of 40 wind turbines with 5 MW and 32 wind turbines with 6.2 MW, with a total capacity of 398.4 MW. Cable J of the double feeders is chosen to transmit the electric energy of the substation to the converter station after cable

**TABLE 5 Wind farm B optimization parameters.**

	Name	Value
Starting position	Length of AC export cables	17067.37 m
	Length of array cables	58630.88 m
	Total cable cost	1,017,775.5 *10 <sup>3</sup> CNY
	Line voltage drop	4.53%
Optimization parameter	Initial step size $l_0$	200 m
	Number of optimization steps	200
Optimal position	Length of AC export cables	14081.51 m
	Length of array cables	57739.89 m
	Total cable cost	955,470.4 *10 <sup>3</sup> CNY
	Line voltage drop	4.32%
Changes	Change in the length of AC export cables	↓2985.86 m
	Change in the length of array cables	↓890.99 m
	Change in the cable cost	↓62,305.1 *10 <sup>3</sup> CNY

**TABLE 6 Wind farm C optimization parameters.**

	Name	Value
Starting position	Length of AC export cables	14029.98 m
	Length of array cables	58311.51 m
	Total cable cost	909,565.9 *10 <sup>3</sup> CNY
	Line voltage drop	4.21%
Optimization parameter	Initial step size $l_0$	180 m
	Number of optimization steps	200
Optimal position	Length of AC export cables	12018.96 m
	Length of array cables	59355.04 m
	Total cable cost	872,744.4 *10 <sup>3</sup> CNY
	Line voltage drop	4.46%
Changes	Change in the length of AC export cables	↓2011.01 m
	Change in the length of array cables	↑1043.53 m
	Change in the cable cost	↓36,821.5 *10 <sup>3</sup> CNY

selection calculation. The values of the related variables during the optimization process are shown in Table 4. At the original location of the wind farm, the path length of the AC export cables is 9727.49 m, the total length of the array cables is 68958.03 m, and the total cost of all cables is 940,476.9 thousand CNY. The optimization starts with an initial step length  $l_0$  of 200 m (the initial step length  $l_0$  is related to the size of the substation, generally taken as three times the longest side length of the substation). As shown in Supplementary Figure S1, during the 200 steps of optimization, there are 26 positions where the total cable cost is lower than the last position. After the optimization, the AC export cable path of the optimal substation location is as shown in Supplementary Figure S2, which is less affected by the

turbine location, and the path is only reduced by 643.78 m after optimization. The array cables at the optimal location are shown in Supplementary Figure S3. Since the change in the substation location is small, the division of the array cable feeders is not affected. The only change is the cable between the substation and the turbine, and the path length is only reduced by 472.33 m. After optimization, the total cable cost of wind farm A decreased by 3,675.7 thousand CNY, a decrease of 0.13%.

#### 4.2.2 Optimization results of wind farm B

Wind farm B consists of 66 wind turbines with 6 MW, with a total capacity of 396 MW. Cable J of the double feeders is chosen to transmit the electric energy of the substation to the converter

station after cable selection calculation. The values of the related variables during the optimization process are shown in Table 5. At the original location of the wind farm, the path length of the AC export cables is 17067.37 m, the total length of the array cables is 58630.88 m, and the total cost of the cable is 1,017,775.5 thousand CNY. With an initial step length  $l_0$  of 200 m, 42 positions in the 200-step optimization process have a total cost of cable lower than the last position, and the optimal substation location is far from the initial position, as shown in Supplementary Figure S4. As shown in Supplementary Figure S5, the AC export cable path of wind farm B is complicated and needs to avoid the wind turbines and not pass through the area of wind farm A. Therefore, the complexity of the search process increases by adopting the Informed-RRT\* method. The optimal substation location and the AC export cable paths change significantly after optimization, with length decreased by 2985.86 m, a decrease of 17.5%. The array cables at the optimal substation location are shown in Supplementary Figure S6, where the optimal location is two turbine units away from the initial position, and the feeder division of the array cables will change accordingly, with length reduced by 890.99 m after the optimization. Due to the significant decrease in the length of the AC export cable path and the array cables after the optimization, the total cost of the cable decreased by 62,305.1 thousand CNY, a decrease of 6.12% for wind farm B.

#### 4.2.3 Optimization results of wind farm C

Wind farm C consists of 78 wind turbines with 4 MW, with a total capacity of 312 MW. Cable K is chosen to transmit the electric energy of the substation to the converter station after the cable selection calculation. The values of the related variables during the optimization process are shown in Table 6. At the starting position, the length of the AC export cable and the array cables are 14029.98 m and 58311.51 m, respectively, and the total cost of the cable is 909,565.9 thousand CNY. Due to the smaller capacity of wind farm C, the size of the substation used is also smaller, with an initial step length  $l_0$  of 180 m for optimization. As shown in Supplementary Figure S7, in the 200-step optimization process, 35 positions have a total cost of cable lower than the last position, and the optimal location is far from the initial position. The path of the AC export cable at the optimal location is shown in Supplementary Figure S8, where the substation moves in the direction of the converter station during the optimization process, with the length reduced by 2011.01 m, a decrease of 14.3%. The array cables at the optimal location are shown in Supplementary Figure S9. The situation of wind farm C is special; after optimizing for the total cost of the cable, the length of the array cables at the optimal location increases by 1043.53 m compared with the initial position. However, considering the decrease in the total cost of the AC export cable, the total cost of the cable for the entire wind farm is reduced by 36,821.5 thousand CNY. This case also illustrates that the length of the AC export cable has a significant impact on the total cost of the cable.

## 5 Conclusion

This paper proposes an integrated optimization method to optimize the path of the OWFCTS, focusing on the optimization of the location of the substation and the optimization of the path of the AC export cables. The research results of this paper are as follows:

- 1) The gradient descent method is applied in the optimization of the location of the substation, which is always optimized in the direction of the gradient descent of the cable cost in the optimization, and at the same time, to avoid the local optimum, the stochastic method is used to jump out of the local optimum when a better value cannot be found. The case of the OWFCTS shows that the method can reduce the cable cost of a large-scale wind farm cluster by 3.58% relative to the starting position, which can effectively improve the economy of wind farm cluster construction.
- 2) Improving the Informed-RRT\* method to optimize the AC export cable path in the OWFCTS, which can identify the wind turbine position and other sensitive areas and avoid them during the optimization process. The case proves that the method can effectively optimize the AC export cable path and find the optimal path, and the optimization of the AC export cable path reaches 13.82% compared with the optimized starting position.

The path integration optimization method of the OWFCTS proposed in this paper can provide technical support and a reference basis for the optimization of the transmission system of the same type of wind farm cluster.

## Data availability statement

The original contributions presented in the study are included in the article/Supplementary Material; further inquiries can be directed to the corresponding author.

## Author contributions

CX: conceptualization and writing–review and editing. ZJ: methodology, validation, writing–original draft, and writing–review and editing. XH: funding acquisition, methodology, and writing–review and editing. YH: visualization and writing–original draft. JW: visualization and writing–original draft. HZ: visualization and writing–review and editing. WS: writing–review and editing.

## Funding

The authors declare financial support was received for the research, authorship, and/or publication of this article. This work was supported by the National Natural Science Foundation of China (grant number 52106238), “the Fundamental Research Funds for the Central Universities” (grant number B230201051), and the Jiangsu Province Policy Guidance Program (International Science and Technology Cooperation/Hong Kong, Macao, and Taiwan Science and Technology Cooperation) (grant number BZ2021019).

## Acknowledgments

The authors would also like to thank their tutors, CX and XH, for their valuable guidance throughout their studies. They provided the tools needed to choose the right direction and successfully complete the dissertation.

## Conflict of interest

The authors declare that the research was conducted in the absence of any commercial or financial relationships that could be construed as a potential conflict of interest.

## Publisher's note

All claims expressed in this article are solely those of the authors and do not necessarily represent those of their affiliated

organizations, or those of the publisher, the editors, and the reviewers. Any product that may be evaluated in this article, or claim that may be made by its manufacturer, is not guaranteed or endorsed by the publisher.

## Supplementary material

The Supplementary Material for this article can be found online at: <https://www.frontiersin.org/articles/10.3389/fenrg.2023.1268291/full#supplementary-material>

## References

- Cazzaro, D., Fischetti, M., and Fischetti, M. (2020). Heuristic algorithms for the wind farm cable routing problem. *Appl. Energy* 278, 115617. doi:10.1016/j.apenergy.2020.115617
- El Mokhi, C., and Addaim, A. (2020). "Optimal substation location of a wind farm using different metaheuristic algorithms," in Proceedings of the 2020 IEEE 6th International Conference on Optimization and Applications (ICOA), Beni Mellal, Morocco, April 2020 (IEEE), 1–6. doi:10.1109/ICOA49421.2020.9094469
- Fischetti, M., and Pisinger, D. (2018). Optimizing wind farm cable routing considering power losses. *Eur. J. Operational Res.* 270 (3), 917–930. doi:10.1016/j.ejor.2017.07.061
- Gammell, J. D., Srinivasa, S. S., and Barfoot, T. D. (2014). "Informed RRT: optimal sampling-based path planning focused via direct sampling of an admissible ellipsoidal heuristic," in Proceedings of the 2014 IEEE/RSJ international conference on intelligent robots and systems, Chicago, IL, USA, September 2014 (IEEE), 2997–3004. doi:10.1109/IROS.2014.6942976
- Global Wind Energy Council (2022). *Global offshore wind report 2022*. Brussels, Belgium.
- Hou, P., Hu, W., and Chen, Z. (2015). "Offshore substation locating in wind farms based on prim algorithm," in Proceedings of the 2015 IEEE Power and Energy Society General Meeting, Denver, CO, USA, July 2015 (IEEE), 1–5. doi:10.1109/PESGM.2015.7286206
- Liu, W., Li, Q., Wang, X., Zhang, F., Li, L., and Yan, H. (2020). Application status and prospect of VSC-HVDC technology for large-scale offshore wind farms. *Electr. Power* 53 (7), 55–70.
- Lundberg, S. (2003). *Performance comparison of wind park configurations*. Göteborg, Sweden: Department of Electric Power Engineering, Power Electronics and Wind Energy.
- Moon, W. S., Kim, J. C., Jo, A., and Won, J. N. (2014). "Grid optimization for offshore wind farm layout and substation location," in Proceedings of the 2014 IEEE Conference and Expo Transportation Electrification Asia-Pacific (ITEC Asia-Pacific), Beijing, September 2014 (IEEE), 1–6. doi:10.1109/ITEC-AP.2014.6941124
- Shin, J. S., and Kim, J. O. (2016). Optimal design for offshore wind farm considering inner grid layout and offshore substation location. *IEEE Trans. Power Syst.* 32 (3), 2041–2048. doi:10.1109/TPWRS.2016.2593501
- Ulku, I., and Alabas-Uslu, C. (2020). Optimization of cable layout designs for large offshore wind farms. *Int. J. Energy Res.* 44 (8), 6297–6312. doi:10.1002/er.5336
- Wang, R., Ma, D., Li, M. J., Sun, Q., Zhang, H., and Wang, P. (2022). Accurate current sharing and voltage regulation in hybrid wind/solar systems: an adaptive dynamic programming approach. *IEEE Trans. Consumer Electron.* 68 (3), 261–272. doi:10.1109/TCE.2022.3181105
- Wang, R., Sun, Q., Ma, D., and Hu, X. (2020). Line impedance cooperative stability region identification method for grid-tied inverters under weak grids. *IEEE Trans. Smart Grid* 11 (4), 2856–2866. doi:10.1109/TSG.2020.2970174
- World Bank Group (2020). Technical-Potential-for-Offshore-Wind-in-China-Map. Available at: [https://www.esmap.org/esmap\\_offshorewind\\_techpotential\\_analysis\\_maps](https://www.esmap.org/esmap_offshorewind_techpotential_analysis_maps) (Accessed July 25, 2023).
- Yang, B., Liu, B., Zhou, H., Wang, J., Yao, W., Wu, S., et al. (2022). A critical survey of technologies of large offshore wind farm integration: summary, advances, and perspectives. *Prof. Control Mod. Power Syst.* 7 (1), 17. doi:10.1186/s41601-022-00239-w
- Yang, Y., Tang, X., and Xin, Y. (2020). Research on optimal site selection for offshore wind farms substation. *Electr. Power* 53 (7), 24–28+71.
- Zuo, T., Meng, K., Tong, Z., Tang, Y., and Dong, Z. H. (2019). Offshore wind farm collector system layout optimization based on self-tracking minimum spanning tree. *Int. Trans. Electr. Energy Syst.* 29 (2), e2729. doi:10.1002/etep.2729